Journal of Hydrology (2008) 357, 228–242

available at www.sciencedirect.com

ScienceDirect

journal homepage: www.elsevier.com/locate/jhydrol

Soil moisture updating by Ensemble Kalman Filtering in real-time flood forecasting

Jürgen Komma *, Günter Blöschl, Christian Reszler

Institute of Hydraulic and Water Resources Engineering, Vienna University of Technology, Karlsplatz 13/222, A-1040 Wien, Vienna, Austria

Received 22 May 2007; received in revised form 28 April 2008; accepted 5 May 2008

KEYWORDS
Data assimilation;
Ensemble Kalman Filter;
Soil moisture;
Distributed rainfall-runoff model

Summary The aim of this paper is to examine the benefits of updating soil moisture of a distributed rainfall runoff model in forecasting large floods. The updating method uses Ensemble Kalman Filter concepts and involves an iterative similarity approach that avoids calculation of the Jacobian that relates the states and the observations. The soil moisture is updated based on observed runoff in a real-time mode, and is then used as an initial condition for the flood forecasts. The case study is set in the 622 km^2 Kamp catchment, Austria. The results indicate that the updating procedure indeed improves the forecasts substantially. The mean absolute normalised error of the peak flows of six large floods decreases from 25% to 12% (3 h lead time), and from 25% to 19% (48 h lead time). The Nash-Sutcliffe efficiency of forecasting runoff for these flood events increases from 0.79 to 0.92 (3 h lead time), and from 0.79 to 0.88 (48 h lead time). The flood forecasting system has been in operational use since early 2006.

Introduction

Updating methods in real-time flood forecasting have enjoyed wide popularity in the late 1970s and early 1980s with the increasing use of telemetry in the control of water resource systems (Wood, 1980). While numerous national flood forecasting systems have indeed implemented updating procedures (e.g., Gutknecht, 1991), scientific interest soon ebbed off. The reasons may well be as O'Connell and Clarke (1981, pp. 202–203) noted: ''The above discussion suggests that there are still considerable unsolved estimation problems in real-time forecasting, but it is not clear to what extent their solution would result in improved forecasts. It may be more beneficial to seek a better representation of the spatial variation in rainfall and its effect on streamflow response, and in improving the structure of real-time forecasting models than to expend effort in solving estimation problems. Information on where efforts will be best rewarded can only be obtained by feedback from case studies.'' Indeed, distributed modelling and use of radar rainfall have been key topics in hydrologic research in the 1990s (e.g., Grayson and Blöschl, 2000). In the mean

* Corresponding author. Tel.: +43 1 58801 22316; fax: +43 1 58801 22399.
E-mail address: komma@hydro.tuwien.ac.at (J. Komma).

0022-1694/$ - see front matter © 2008 Elsevier B.V. All rights reserved.
doi:10.1016/j.jhydrol.2008.05.020

time, updating methods have been developed along a separate avenue where the interest resided in how to best use soil moisture satellite data in hydrological models to improve climate forecasts (McLaughlin, 1994). In this context, updating is usually referred to as data assimilation. Methods have been gleaned from oceanography and atmospheric sciences (Reichle et al., 2002) rather than from control theory as had been the case in the earlier flood forecasting research. The availability of new methods has kindled renewed interest in the updating problem of flood forecasting. Specifically, Monte Carlo methods are appealing because of their flexibility, case of use and operational robustness (Madsen and Skotner, 2005). The Ensemble Kalman Filter (Evensen, 1994) extends the traditional Kalman Filter (Kalman, 1960) concept by Monte Carlo techniques and is able to deal with non-linear model dynamics in a natural way without linearised model equations. Moradkhani et al. (2005) found that the updating procedure improved runoff forecasts of a conceptual hydrologic model when using on-line measured runoff. Weerts and Serafy (2006) compared the performance of three methods of updating a conceptual runoff model — Ensemble Kalman Filtering, particle filtering and residual resampling. They suggested that the Ensemble Kalman Filter technique was the most efficient method in case of a small number of realisations, and was generally more robust than the other methods. The Ensemble Kalman Filter is hence an obvious choice for updating flood forecasts.

The aim of this paper is to examine the benefit of an updating method that is based on Ensemble Kalman Filter concepts in forecasting large floods. Using observed runoff, the soil moisture state of the catchment is updated which is then used as an initial condition for the forecasts. The analysis is based on a distributed rainfall-runoff model in the Kamp catchment in Austria that is part of a flood forecasting system that has been in operational use since early 2006.

Data and methods

Study catchment and data

The Kamp catchment is located in northern Austria, approximately 120 km north-west of Vienna. At the Zwettl stream gauge the catchment size is 622 km^2 and elevations range from 500 to 1000 m a.s.l. The higher parts of the catchment in the Southwest are hilly with deeply incised channels. Towards the catchment outlet in the Northeast the terrain is flatter and swampy areas exist along the streams. Typical flow travel times in the river system range from 2 to 4 h. The geology of the catchment is mainly granite and gneiss. Weathering has produced sandy soils with a large storage capacity throughout the catchment. A catchment fraction of 50% is forested. Mean annual precipitation is about 900 mm of which about 300 mm becomes runoff (Parajka et al., 2005c). During flood events, only a small proportion of rainfall contributes to runoff. Typically, the event runoff coefficients are 10% or less (Merz and Blöschl, 2005). As rainfall increases in magnitude, the runoff response characteristics change fundamentally because of the soil moisture changes in the catchment and the runoff coefficients can easily exceed 50%. The catchment is hence highly non-linear in its rainfall-runoff response. Representing catchment soil moisture well is hence of utmost importance for producing accurate flood forecasts.

For the development of the distributed model, data from a total of 16 rain gauges were used. Out of these, 10 rain gauges recorded at a time interval of 15 min, the others were daily gauges. Eight of the recording rain gauges are telemetered (Fig. 1) and are used for the operational forecasting. At each time step, the rain gauge data are spatially interpolated to a 1 km grid, supported by climatologically scaled radar information. While the operational system uses rainfall forecasts, all analyses in this paper are based on the assumption that future rainfall were known from the rain gauge data to focus on the value of the updating procedure in reducing forecasting errors.

Hydrologic model

The model used in this paper is a spatially-distributed continuous rainfall-runoff model (Reszler et al., 2006 and Blöschl et al., 2008). The model runs on a 15 min time step and consists of a snow routine, a soil moisture routine and a flow routing routine. The snow routine represents snow accumulation and melt by the degree-day concept. The soil moisture routine represents runoff generation and changes in the soil moisture state of the catchment and involves three parameters: the maximum soil moisture storage L_s, a parameter representing the soil moisture state above which evaporation is at its potential rate, termed the limit for potential evaporation L_P, and a parameter in the non-linear function relating runoff generation to the soil moisture state, termed the non-linearity parameter β. The details of the soil moisture routine are given in Appendix A. Runoff routing on the hillslopes is represented by an upper and two lower soil reservoirs. Excess rainfall Q_p enters the upper zone reservoir and leaves this reservoir through three paths, outflow from the reservoir based on a fast storage coefficient k_1; percolation to the lower zones with a percolation

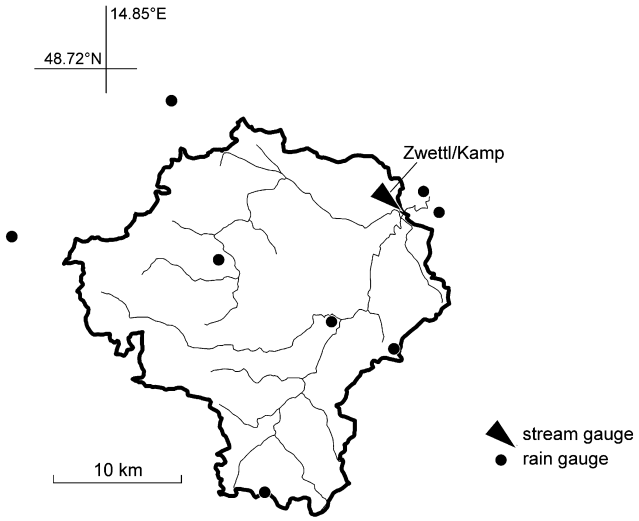

Figure 1 Kamp catchment (622 km^2) with telemetered rain gauges and stream gauge shown. Thick line represents the catchment boundary, thin lines the river network.

rate c_P; and, if a threshold of the storage state L_1 is exceeded, through an additional outlet based on a very fast storage coefficient k_0. Water leaves the lower zones based on the slow storage coefficients k_2 and k_3. Bypass flow Q_{by} is accounted for by recharging the lower zone reservoir (k_2) directly by a fraction of the excess rainfall. k_1 andk_2 as well as c_P have been related to the soil moisture state in a linear way. The outflow from the reservoirs represents the total runoff Q_t on the hillslope scale. These processes are represented on a 1 km $\times$ 1 km grid. The model states for each grid element are the snow water equivalent, soil moisture S_s of the top soil layer, the storage of the soil reservoirs S_1, S_2 and S_3 associated with the storage coefficients k_1, k_2 and k_3, with $k_1 < k_2 < k_3$. The model parameters for each grid element were identified based on the 'dominant processes concept' of Grayson and Blöschl (2000) which suggests that, at different locations and different points in time, a small number of processes will dominate over the rest. Land use, soil type, landscape morphology (e.g., the degree of incision of streams) and information on soil moisture and water logging based on field surveys were used. Discussions with locals provided information on flow pathways during past floods. Runoff simulations, stratified by time scale and hydrological situations, were then compared with runoff data, and the simulated subsurface dynamics were compared with piezometric head data. The various pieces of information were finally combined in an iterative way to construct a coherent picture of the functioning of the catchment system, on the basis of which plausible parameters for each grid element were chosen. The model was extensively tested against independent runoff data both at the seasonal and event scales. Data from 1993 to 2003 were used for model identification and parameter calibration. Data from 2004 to 2006 were used for model verification.

Runoff routing in the stream network is represented by cascades of linear reservoirs with parameters n (number of reservoirs) and k (storage coefficient) that are a function of runoff. Decreasing travel times with increasing flood levels are represented by linearly decreasing k with runoff over a certain range but as the flood water exceeds bank full runoff, k is decreased to represent flood attenuation on the flood plains. The model parameters for each reach have been found by calibration against observed hydrographs and results of hydro-dynamic simulation models. The effect of stream routing on the runoff hydrograph is relatively small as compared to runoff generation within the catchment, so most of the effort was devoted to obtaining a realistic representation of catchment processes. All model equations have been implemented in state-space notation to facilitate use of the Ensemble Kalman Filter.

Ensemble Kalman Filter

The idea of the Kalman Filter is to provide an estimate of a state vector based on model information and measurement information, balancing out the errors of the two. It is a sequential algorithm for minimising the state error variance. While one would usually choose soil moisture as the state vector in runoff forecasting, an alternative approach is proposed in this paper. Runoff is treated as if it were a state vector and is updated based on runoff data in real time. For consistency with the usual notation (e.g., Madsen et al., 2003) runoff is denoted by x here. The measurement error is attributed to the error in runoff measurements, the model error to the error in precipitation and evaporation input. In the Ensemble Kalman Filter, the model $\Phi(\cdot)$ is now applied to each of the M members of the ensemble to estimate the runoff:

$$x^f_{m,i} = \Phi(x^a_{m,i-1}, u_i + \varepsilon_{m,i}), \quad m = 1, 2, \ldots, M \tag{1}$$

where $x_{m,i}$ is the runoff of ensemble member m at time step i, $x_{m,i-1}$ is the runoff at the previous time step, superscript f stands for forecast, superscript a stands for analysed, u_i is the model input (precipitation, evaporation) and $\varepsilon_{m,i}$ is the model error which is randomly drawn from a normal distribution with zero mean and model error covariance $\mathbf{V}_i$. As an *a priori* forecast, the mean value of the ensemble forecasts is adopted:

$$x^f_i = \overline{x^f_i} = \frac{1}{M}\sum_{m=1}^{M} x^f_{m,i} \tag{2}$$

The error covariance matrix $\mathbf{P}^f_i$ of the forecast is estimated from the ensemble forecasts as:

$$\mathbf{P}^f_i = \mathbf{S}^f_i (\mathbf{S}^f_i)^T \tag{3}$$

with

$$s^f_{m,i} = \frac{1}{\sqrt{M-1}}(x^f_{m,i} - \overline{x^f_i}) \tag{4}$$

where $s^f_{m,i}$ is the mth column of $\mathbf{S}^f_i$. In a next step, the measurements z_i of runoff are contaminated by a measurement error $\eta_{m,i}$ to generate an ensemble of M possible measurements:

$$z_{m,i} = z_i + \eta_{m,i}, \quad m = 1, 2, \ldots, M \tag{5}$$

where $\eta_{m,i}$ is randomly drawn from a normal distribution with zero mean and covariance $\mathbf{W}_i$. Each ensemble member $x^f_{m,i}$ is then updated according to

$$x^a_{m,i} = x^f_{m,i} + \mathbf{K}_i(z_{m,i} - \mathbf{C}_i x^f_{m,i}) \tag{6}$$

where $\mathbf{K}_i$ is the Kalman gain:

$$\mathbf{K}_i = \mathbf{P}^f_i \mathbf{C}^T_i [\mathbf{C}_i \mathbf{P}^f_i \mathbf{C}^T_i + \mathbf{W}_i]^{-1} \tag{7}$$

and $\mathbf{C}_i$ is the Jacobian matrix that relates the measurements and the state vector. Based on the updated ensemble members, the updated a posteriori estimates of the state vector x^a_i and the error covariance matrix $\mathbf{P}^a_i$ are calculated analogously to (2) and (3).

To illustrate the dynamics of the Ensemble Kalman Filter for a simple case, Fig. 2 shows a comparison of updated outflows from a linear reservoir using the original Kalman Filter (KF) and the Ensemble Kalman Filter (EnKF) with ensemble sizes of $M = 10$ and 100. The model equation is $x_i = \kappa \cdot x_{i-1}$ with the recession parameter chosen as $\kappa = 0.9$, the measurement error variance W and the model error variance Vboth chosen as 0.5 $(m^3/s)^2$ and the initial flow chosen as $x_0 = 1$ m^3/s. The example can be interpreted as the recession of a flood hydrograph. Again for illustrative purposes, it was assumed that runoff measurements are available every seventh time step. As the measurements become available, the estimation variance of the Kalman Filter

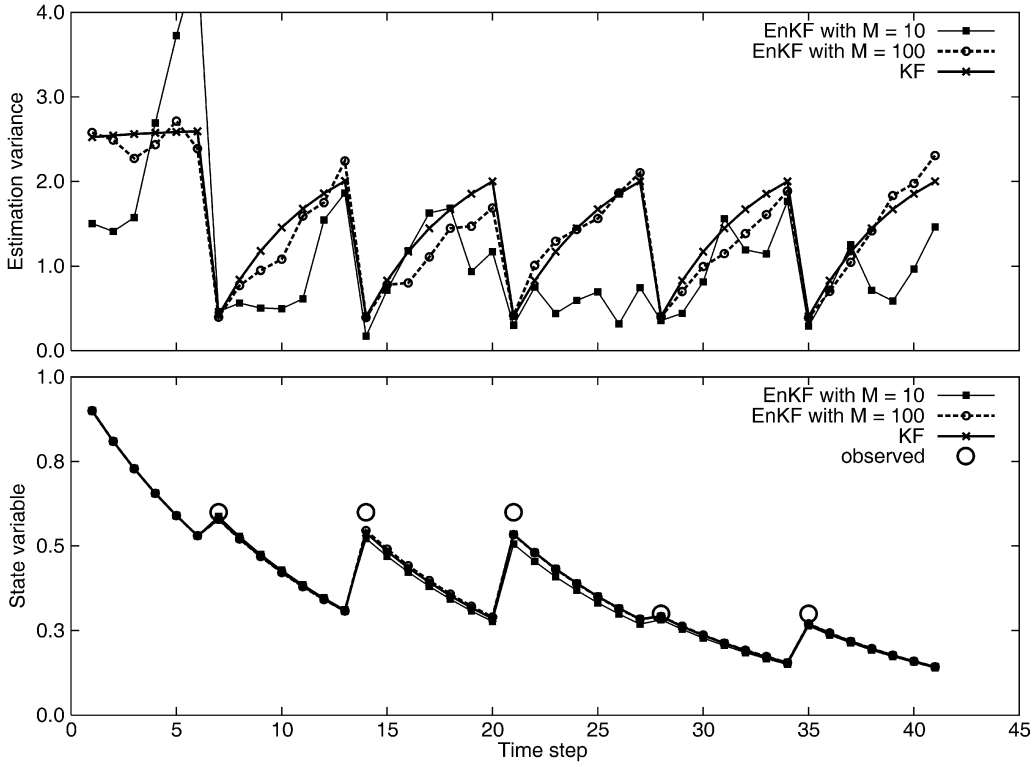

Figure 2 State variable (i.e., runoff) and estimation variance for the recession from a linear reservoir estimated by the Kalman Filter (KF) and the Ensemble-Kalman-Filter (EnKF) making use of runoff data at intervals of 7 time steps. *M* is the ensemble size (i.e., the number of realisations).

decreases to about 0.4 and increases as the system loses the memory of that information. The degree to which the Ensemble Kalman Filter matches the pattern of the estimation variance depends on the size *M* of the ensemble. While for $M = 10$ the patterns is not represented well, for $M = 100$ the match is much closer. Of course, in the limit of $M \rightarrow \infty$, the results of the Ensemble Kalman Filter should approach those of the Kalman Filter for this simple linear case. The estimated state variable (i.e., runoff) is adjusted as the runoff measurements become available (lower panel of Fig. 2). In contrast to the estimation variance, the estimated state variable is represented well for an ensemble size as small as 10. This is hardly surprising in the light of the efficiency of the method pointed out by Weerts and Serafy (2006), but nevertheless satisfying for the purposes of flood forecasting. While the flood forecasting model is non-linear, so the efficiency of the estimates will be different, the simple comparison does point to an order of magnitude of the ensemble size needed of $M = 10$, if the main interest lies in representing the state variable (i.e., runoff) well.

There are a number of possibilities for implementing the Ensemble Kalman Filter with a flood forecasting model that are related to formulating the errors and the states. One can separately represent different sources of the model error by different error terms. The advantage of doing this is that the physical basis of individual error sources remains clear. For example, one can separately represent errors in precipitation estimation, evaporation, as well as errors in model structure and model parameters. While the separate representation of many error sources is conceptually appealing it may be difficult in a practical application to specify the error distribution for each of the sources in a reliable way. If the model error assumptions are inappropriate, the updating may degrade the model performance as compared to the case without updating, as illustrated by Crow and Van Loon (2006) for the case of assimilating remotely sensed surface soil moisture. Also, some of the errors are likely correlated and, if the approach of separately representing component errors were adopted one would also have to account for these interrelationship. In this paper we have hence chosen to represent the errors in precipitation and evaporation input as the model error in an aggregate way, both for simplicity and parsimony.

In terms of formulating the states one possibility is a dual-state scheme. However, dual-state schemes may, potentially, give rise to identifiability issues. For example, Crow and Van Loon (2006) found that it was difficult to estimate two states (surface soil moisture and root zone soil moisture) from remote sensing data of surface soil moisture alone. As a remedy they recommended dual assimilation of both runoff observations and surface soil moisture observations (from remotely sensed data) that may allow more robust estimates of the two states. Dual assimilation of runoff observations and surface soil moisture observations would also be a possibility here but Parajka et al. (2005b) demonstrated that very little can be gained in terms of runoff prediction capabilities when assimilating remotely sensed soil moisture in Austria. While in this paper the suitability of a dual-state scheme has not been tested, a single-state scheme was hence considered a robust choice. The main

idea of the approach chosen here is that runoff is treated as if it were a state vector and is updated based on runoff data in real time according to Eq. (6). The main advantage of doing this is that $\mathbf{C}_i$ in (7) then is the identity matrix and there is no need to calculate it. The updated a posteriori runoff x_i^a represents an updated estimate of the current runoff considering uncertainties of the model results and the runoff measurements. Therefore the updated runoff x_i^a provides a logical basis for the real-time flood forecast at the current time step i. However, the catchment soil moisture S_s, and the storage of the soil reservoirs S_1, S_2 and S_3 of each grid element associated with x_i^a are unknown as they are propagated forward in time according to the non-linear model equations while x_i^a is estimated directly from Eq. (6). To run the model in a forecast mode from the updated initial conditions, soil moisture and the storage of the soil reservoirs are required. They are also required for the forward propagation of the estimation covariance derived from the runoff ensemble. While in the classical Kalman filter one would obtain soil moisture by the Jacobian matrix $\mathbf{C}_i$ in Eq. (7), as an alternative, a simple similarity approach is adopted here to find soil moisture and the storage of the soil reservoirs of each pixel that is consistent with the a posteriori runoff x_i^a. For each ensemble member m, a set of N additional realisations is generated by forward propagation of the hydrologic model Φ which is the runoff model as presented in Blöschl et al. (2008):

$$x_{n,m,i}^f = \Phi(x_{n,m,i-1}^f, u_i + \varepsilon_{n,i}), n = 1, 2, ..., N \quad (8)$$

adding random errors $\varepsilon_{n,i}$ of precipitation and evaporation that are spatially uniform. These realisations are termed auxiliary realisations while the ensemble of $m = 1$, M contains the main realisations. The auxiliary realisations start from a time step where soil moisture and the storage of the soil reservoirs are known. At time step j the auxiliary realisations $x_{n,m,i}^f$ differ because of the random errors. One of the auxiliary realisations $x_{n,m,i}^f$ is closest to the a posteriori runoff $x_{m,i}^a$. This realisation $x_{n,m,i}^f$ is assumed to be consistent with $x_{m,i}^a$, i.e.,

$$|x_{m,i}^a - x_{n,m,i}^f| \rightarrow \min \quad (9)$$

which gives the soil moisture and the storage of the soil reservoirs for all grid elements at time i for each realisation m.

As the initial conditions of the real-time forecasts the realisation m is selected that is closest to the mean value of all realisations in terms of runoff, i.e.,

$$|\overline{x_i^a} - x_{m,i}^a| \rightarrow \min \quad \text{with} \quad \overline{x_i^a} = \frac{1}{M}\sum_{m=1}^{M} x_{m,i}^a \quad (10)$$

A schematic overview of the real-time model update with Ensemble Kalman Filter concepts and the similarity approach is given in Fig. 3. The current time step is labelled i and the time increment is 1. Tests with the procedure suggested that it is useful to start the realisations at u time intervals before time step i for numerical reasons. Fig. 3a shows three ensemble members of the Ensemble Kalman Filter with their respective values $x_{1,i}^f$, $x_{2,i}^f$, and $x_{3,i}^f$ at time step i. They approximate the probability density function (pdf) of the a priori estimates (dashed dotted line in Fig. 3a). The perturbed observations $z_{1,i}$, $z_{2,i}$ and $z_{3,i}$ that approximate the pdf of the observation errors (dotted line in Fig. 3a) are combined with the $x_{1,i}^f$, $x_{2,i}^f$ and $x_{3,i}^f$ by Eq. (6) to obtain the $x_{1,i}^a$, $x_{2,i}^a$ and $x_{3,i}^a$ which approximate the pdf of the a posteriori estimates (solid line in Fig. 3a). In the schematic of Fig. 3, the Kalman gain has been chosen as $K_i = 0.6$. To obtain the soil moisture and the storage of the soil reservoirs of each pixel, auxiliary realisations are started at time step $i - u$. In Fig. 3b, $N = 3$ auxiliary realisations are shown for the main realisation $m = 1$ which produce $x_{1,1,i}^f$, $x_{2,1,i}^f$ and $x_{3,1,i}^f$. In the schematic, the auxiliary realisation $n = 3$ is the one that is closest to the a posteriori estimate of realisation $m = 1$ as $|x_{1,i}^a - x_{3,1,i}^f|$ is small. The soil moisture and the storage of the soil reservoirs of each pixel associated with the auxiliary realisation $n = 3$ is hence used to represent the a posteriori estimate of realisation $m = 1$. For the example in Fig. 3 the initial conditions for the a posteriori estimate$x_{2,i}^a$ are used for the forecasts according to Eq. (10).

Application of the Ensemble Kalman Filter concepts to the Kamp catchment

The soil moisture and the storage of the soil reservoirs of the grid elements of the hydrologic model at the beginning of a flood event are clearly important for reliable flood

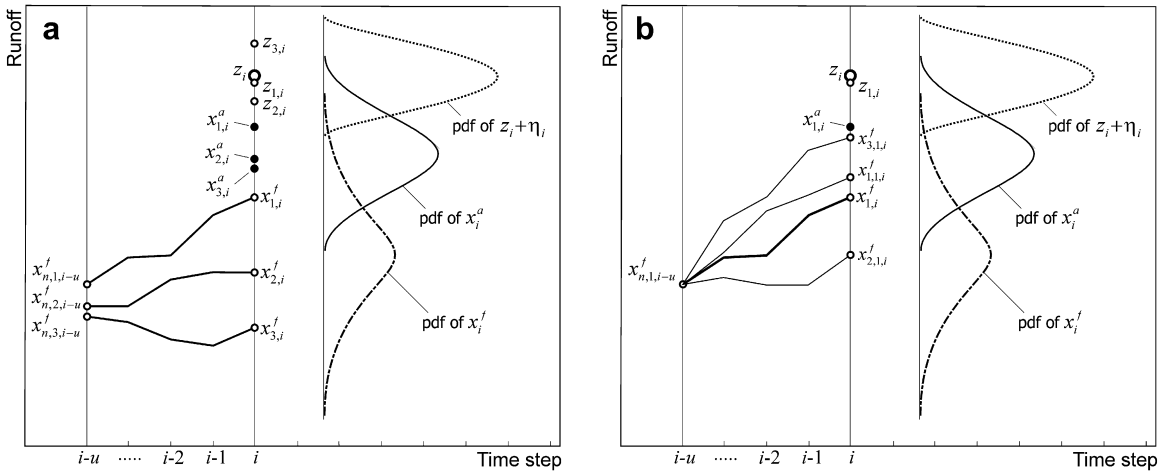

Figure 3 (a) Schematic of the Ensemble Kalman Filter approach. (b) Schematic of the similarity approach. For symbols see text.

forecasts. If the initial system state deviates from the optimal state, the flood forecasts will also be less than perfect. An overestimation of soil moisture at the beginning of a flood event would be expected to lead to an overestimation of the observed flood peak and, in a similar way, an underestimation of soil moisture would cause an underestimation of flood peaks. Biases in the soil moisture may be the result of small biases in the input, i.e., precipitation and evapotranspiration, that may accumulate over weeks and months. It is these biases the updating procedure of this papers aims to correct. While updating methods commonly used in real-time flood forecasting (e.g., Gutknecht, 1991) update runoff generation during events, the procedure presented here updates the evolution of soil moisture between events by attributing the model uncertainty to rainfall and evapotranspiration inputs. This means, it is the slow component of soil moisture change in the catchment that is adjusted. The model error variance must hence be set to reflect the slow processes. As there is a single stream gauge, the covariances simplify to scalar variances.

In order to find suitable parameters for the updating procedure we performed extensive test calculations with different sets of parameters and different error models (white and red noise) for time periods including floods and low flow conditions. Based on the results of these calculations, the model variances for the ensemble of main and auxiliary realisations are set to $V_i = 0.005$ $(\text{mm}/15\ \text{min})^2$. As the variance of the sum of independent random variables scales with the number of aggregation steps, this value is equivalent to an error standard deviation of 1.8 mm/week (with a time step of 0.25 h). This is the order of magnitude one would expect for the uncertainty of the precipitation measurements and estimation of evaporation, although it is difficult to separate the individual effects. It is clear that this magnitude relates to the small biases over a relatively long time period rather than to precipitation errors during a flood event which could be much larger. The small model variance updates the system states between the flood events to improve the initial conditions for the forecasts of future flood events.

The accuracy of runoff measurements tends to decrease with increasing runoff. Typically, the error standard deviation is set to a fixed percentage of runoff. The measurement error variance of runoff was hence formulated as $W_i = \xi \cdot z_i^2$. Again based on test simulations, ξ was set to $\xi = 0.0025$. Runoff measurement errors depend on the sampling method and on the local stream geometry but, typically, the error standard deviations are on the order of 5% of the runoff (Herschy, 2002). This means that the measurement error variance used here is the order of magnitude one would expect for the uncertainty of the runoff measurements.

One of the advantages of the Ensemble Kalman Filter is its flexibility with regards to the statistical characteristics of the model and measurement errors. During the parameterisation of the update procedure test calculations with red noise (i.e., temporally correlated) model errors were carried out. The test calculations indicated that for the red noise case, larger ensemble sizes M are needed than in the white noise case to get similar results. White noise error terms without a correlation in time were hence used for the model and measurement errors. As there is a single stream gauge, $\mathbf{C}_i = C_i = 1$.

Test simulations were performed to determine a suitable ensemble size. For a given time period the updating procedure was run with a large ensemble size and the ensemble size was gradually reduced, similar to Fig. 2. These comparisons suggested that an ensemble size of $M = 10$ gives very similar estimates of runoff to the case of large ensemble sizes with less than 1% difference. $M = 10$ was hence adopted in this case study. N was set to $N = 10$ in a similar comparison. The update interval was set to $u = 12$. With a time step of $\Delta t = 0.25$ h the update interval Δt_u is hence 3 h. This lag is needed because of the non-linearity — any additional rainfall will not immediately produce a response at the catchment outlet as there is some time lag within the catchment. Table 1 summarises the parameters of the updating procedure used in this paper.

Sensitivity to soil moisture

The way the updating procedure operates in the Kamp model is illustrated in two scenarios (Figs. 4 and 5). To emulate the situation in real-time flood forecasting, the update of the system states is only performed during the low flow period before the first rise of the hydrograph on October 20, which would be the past in a forecast situation. From October 20 (which would be the future), the simulation is performed without any updating and observed precipitation from rain gauges is used as a model input for clarity. In Fig. 4, the initial soil moisture at the beginning of the calculation period was set to 0%, i.e., the top soil was assumed to be perfectly dry. Shown in the graphs is the mean value of the relative soil moisture within the catchment

$$\overline{S_s/L_s} = \frac{1}{n_p} \cdot \sum_{k=1}^{n_p} \frac{S_{s_k}}{L_{s_k}} \tag{11}$$

where S_{s_k} and L_{s_k} are the simulated soil moisture and their limit at grid element k. n_p is the number of grid elements

Table 1 Parameters of the Ensemble Kalman Filter

Parameter	Symbol	Unit	Value
Time step	Δt	h	0.25
Updating time step	Δt_u	h	3
Measurement error variance of runoff	W_i	$(\text{m}^3/\text{s})^2$	$\xi \cdot z_i^2, \xi = 0.0025$
Model error variance	V_i	$(\text{mm}/15\ \text{min})^2$	0.005
Ensemble size	M		10
Auxiliary ensemble size	N		10

z_i is measured runoff.

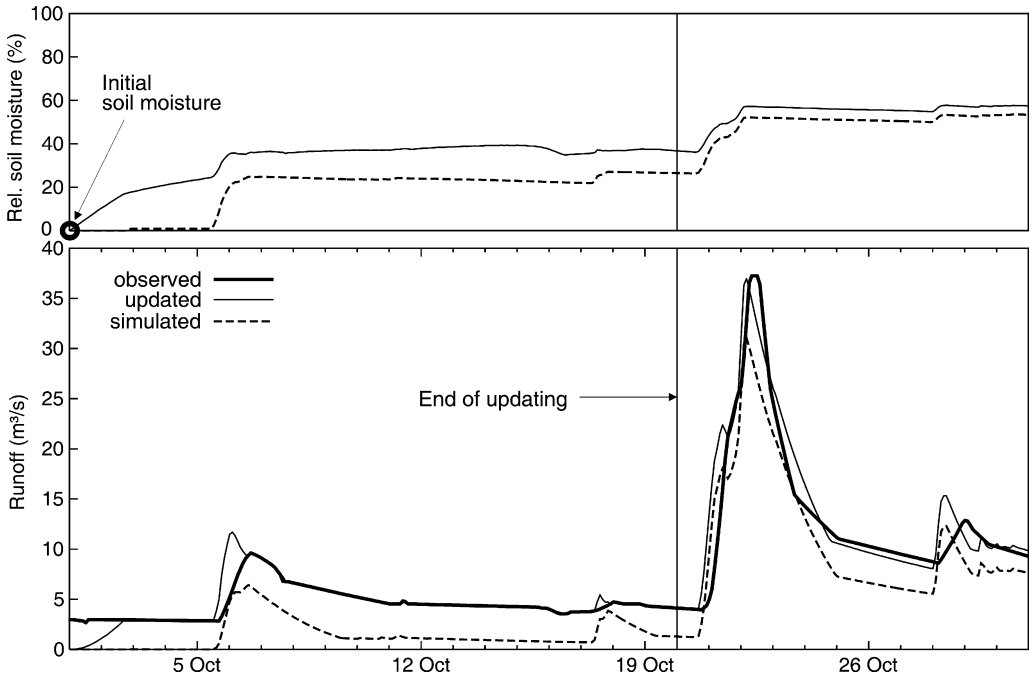

Figure 4 Scenario with initial soil moisture set to an arbitrary low value to illustrate the effect of updating by the Ensemble Kalman Filter on mean relative soil moisture $\overline{S_s/L_s}$ and runoff. October 1996, stream gauge Zwettl/Kamp.

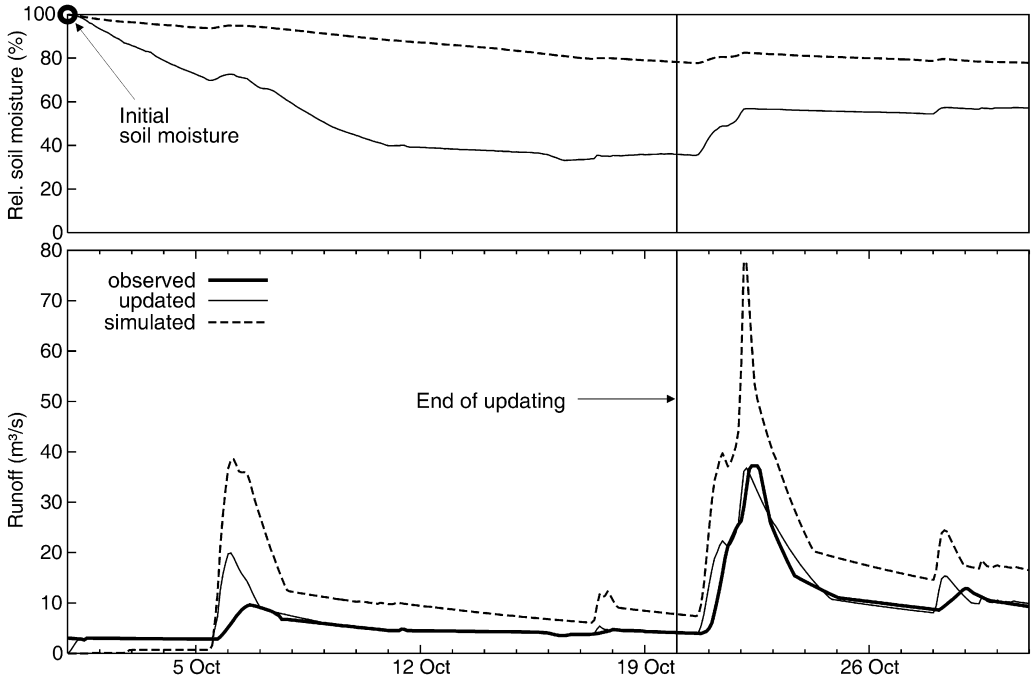

Figure 5 Scenario with initial soil moisture set to an arbitrary large value to illustrate the effect of updating by the Ensemble Kalman Filter on mean relative soil moisture $\overline{S_s/L_s}$ and runoff. October 1996, stream gauge Zwettl/Kamp.

with $n_P = 622$. In a simulation mode without updating (dashed lines) the model consistently underestimates soil moisture and hence runoff. When updating is allowed (thin solid lines) the model adjusts the perceived errors in precipitation and evaporation and hence increases soil moisture more quickly than in the simulation case. The updating of the model input affects the entire hydrologic system including the storage of the soil reservoirs not shown. The updated runoff hence reaches the level of the observed hydrograph after a short time period. In case of the simulation without updating, the flood peak on October 23 is clearly underestimated while the forecast that uses updated initial

conditions (thin solid lines) is much closer to the observed hydrograph. As noted above, it is antecedent soil moisture that is aimed to be improved on by the updating procedure.

A similar scenario, but with very wet initial conditions is shown in Fig. 5. The effect of the updating is similar in that it adjusts the soil moisture to a reasonable value. Without updating the flood peak is vastly overestimated as a consequence of the overestimated soil moisture at the beginning of the flood event. A comparison of Figs. 4 and 5 indicates that, in both cases, updated soil moisture converges to a value that is consistent with runoff. On October 20 (i.e., the hypothetical time of the forecast) soil moisture in both Figs.

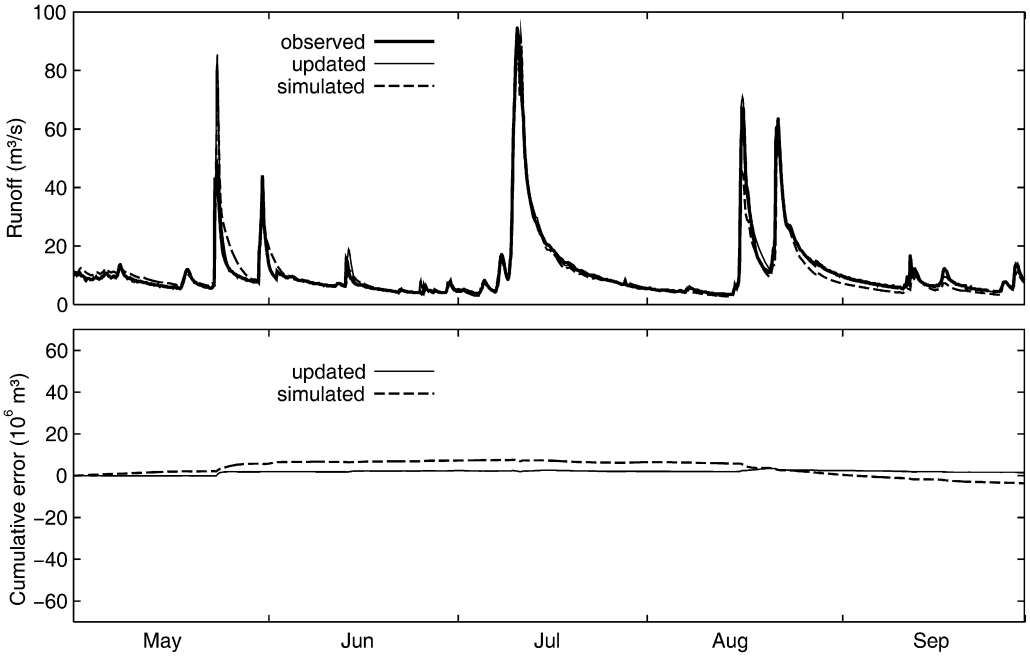

Figure 6 Simulations without updating (dashed lines) and updating (thin solid lines) of runoff (top) and cumulative errors (bottom) at Zwettl/Kamp from May to September 2005. Example of excellent model performance where the benefits of updating are small.

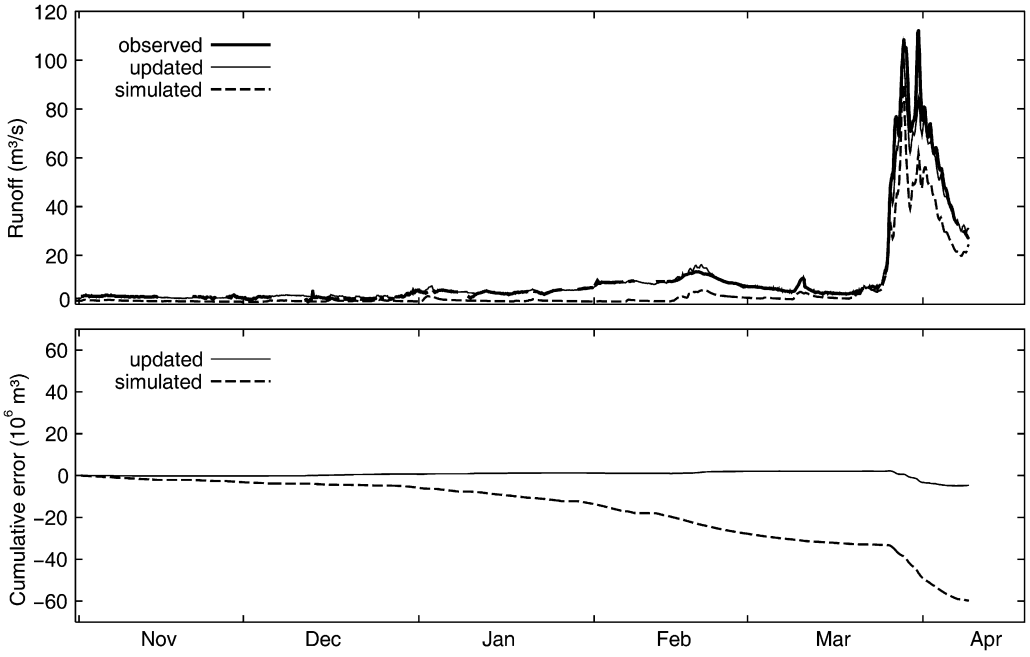

Figure 7 Simulations without updating (dashed lines) and updating (thin solid lines) of runoff (top) and cumulative errors (bottom) at Zwettl/Kamp from November 2005 to April 2006. Example of poor model performance where the benefits of updating are significant.

4 and 5 was 38%, while without updating, it was 23% and 79%, respectively.

The scenarios illustrate that accurate estimates of antecedent soil moisture are indeed of utmost importance for producing accurate forecasts. Inadequate initial moisture can be corrected and suitable moisture conditions can be estimated by updating the model input during the dry period before the flood event on October 23.

Results

Updating soil moisture in a simulation mode

Fig. 6 shows the results of simulation runs with and without model update from May to September 2005. The calculation results with model update are simply the analysed state estimates x_i^a. During this period, the simulation without updating performs very well. Both the shape and the peaks of the simulated flood hydrographs are close to the observations. The cumulative errors (lower part of Fig. 6) are very small. The cumulative error never exceeds 7×10^6 m^3 within this period which is small as compared to the total flow volume of 140×10^6 m^3. This is because of the favourable model performance. There is a slight improvement in the May event and the August events, but overall there is hardly any difference between the simulations with and without updating. This example is the ideal case for real-time flood forecasting, where the model performs well in the simulation mode, so one would also expect the model to work well in the forecasts.

An alternative example is shown in Fig. 7 for the period from November to April 2006. Until the end of December the simulated hydrograph is slightly lower than the data. This is most likely due to uncertain precipitation and evaporation inputs during this relatively dry period. From January until the end of March the differences between simulation and observation increases which is reflected in a progressive increase in the negative cumulative errors. During this period the likely reason for this underestimation are the uncertainties in simulating snow accumulation and snow melt. The effect of these biases is the underestimation of the soil moisture at the beginning of the flood event in April 2006. As a result, the entire flood event in April is substantially underestimated. In contrast, the simulation with updating performs much better during the low flow period until the end of March. The antecedent soil moisture at the beginning of the flood event in April is larger than for the simulation case without updating and the flood event is represented much more accurately. For this example, the advantage of the updating during the low flow period is obvious.

Updating soil moisture in a forecast mode

The examples in Figs. 6 and 7 were illustrative of the merits of updating, depending on the performance of the simulation per se. In a forecast situation, however, the updating is for the past only. The forecast starts with the updated initial conditions but, of course, with no additional updating of the forecast as future runoff data are not available. This situation is illustrated in Figs. 8 and 9. Up to the time the forecast is made (vertical lines in Figs. 8 and 9), the updating is as in Figs. 6 and 7 but beyond that point in time no more updating is allowed although future precipitation is assumed

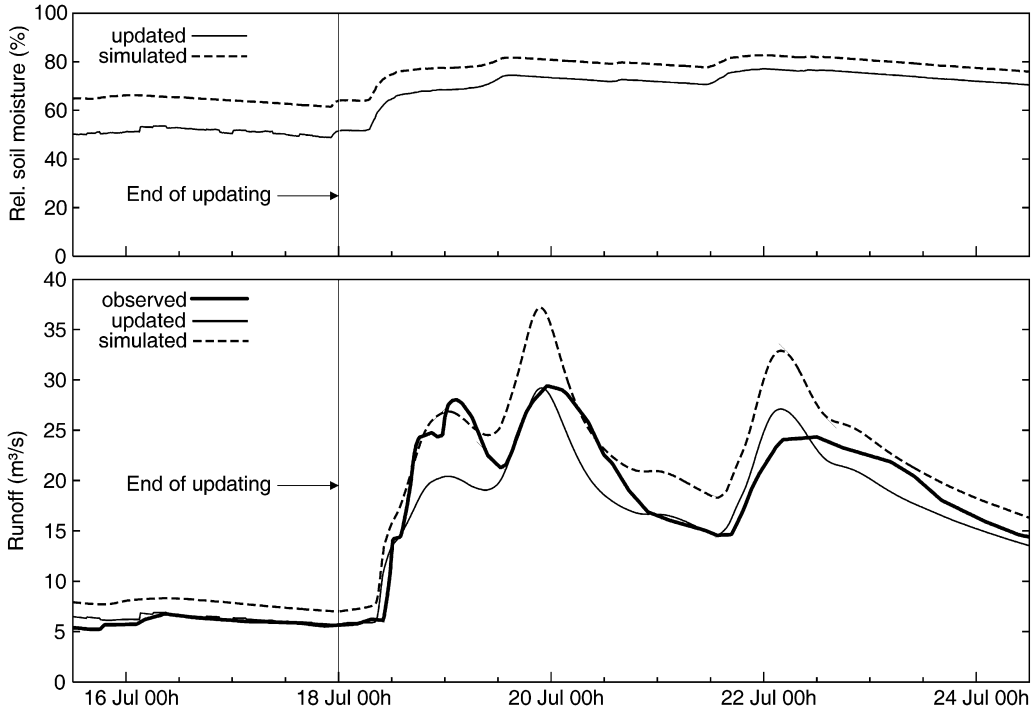

Figure 8 Effect of updating soil moisture in the forecast mode. The forecast was started from simulated and updated initial conditions on 18 July 1997 at 0 h. Future precipitation is assumed to be known but no updating is performed beyond the forecast time (vertical line). Zwettl/Bahnbrücke (622 km^2).

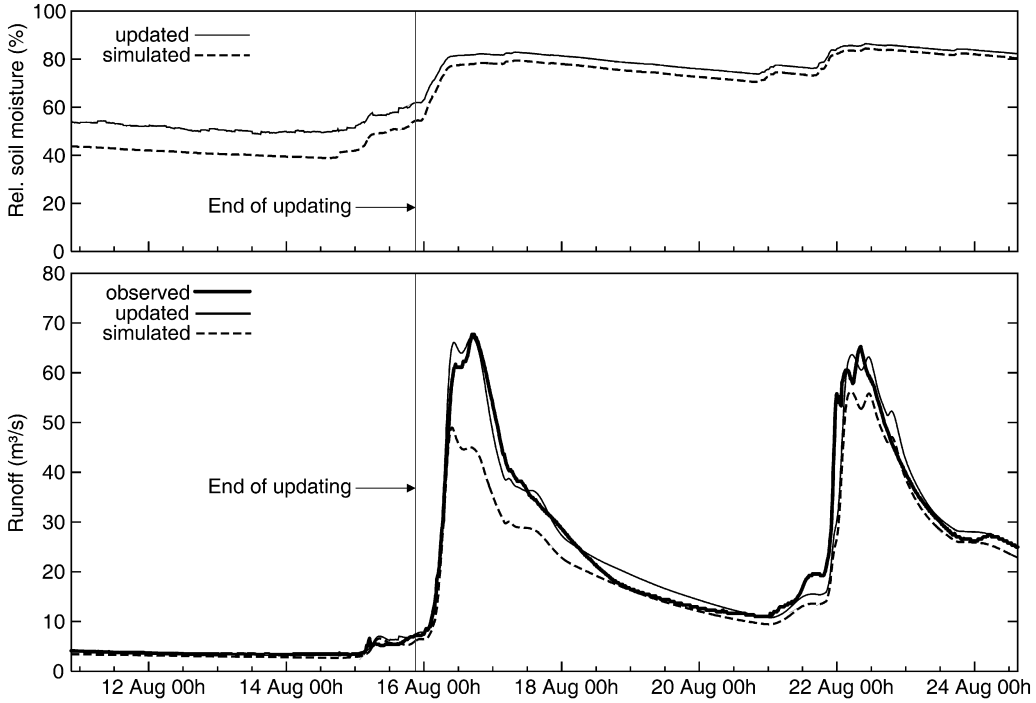

Figure 9 Effect of updating soil moisture in the forecast mode. The forecast was started from simulated and updated initial conditions on 15 August 2005 at 21 h. Future precipitation is assumed to be known but no updating is performed beyond the forecast time (vertical line). Zwettl/Bahnbrücke (622 km^2).

to be known. The difference between the updating and no updating (simulation) cases in Figs. 8 and 9 for the points in time later than the forecast time is hence only related to the difference in the initial conditions at the forecast time.

The upper panel of Fig. 8 shows simulated and updated mean relative soil moisture $\overline{S_s/L_s}$, the lower panel shows the associated hydrographs. During July 16 and 17 before the start of the event, runoff is overestimated in the simulation (no updating) case because soil moisture and the storage of the soil reservoirs are overestimated as a result of biases accumulated over the previous months. The updating brings soil moisture and the storage of the soil reservoirs as well as runoff down, so that runoff is very similar to the data. At the time the forecast is made, relative soil moisture is 62% and 51% in the simulation and updating cases, respectively. These are the initial conditions for the forecasts along with the storage of the soil reservoirs S_1, S_2 and S_3 not shown. The forecast based on the simulated initial conditions overestimates the observed hydrograph during most of the forecast lead time (19—22 July). The forecast based on the updated initial conditions does underestimate the first peak but performs substantially better for the remaining forecast lead time. Fig. 8 is an example where soil moisture (without updating) is overestimated prior to the event which is quite apparent in the overestimation of runoff. Fig. 9 shows the converse example where soil moisture (without updating) is underestimated prior to the event but this is not so obvious in the hydrograph. In fact, the simulated initial runoff is only slightly lower than the measurement but the flood peak of the following event is clearly underestimated by the simulation. In this example, the updated initial soil moisture improves the forecast accuracy very substantially which is due to the updating of soil moisture during the dry period before the flood event. It is interesting that the non linearity of the rainfall-runoff model amplifies the small differences in runoff prior to the event. This means that small differences between simulated and observed hydrographs can have a great effect on the runoff forecast. Conversely, these small differences can be exploited to improve the forecasts. It is also interesting that the difference in soil moisture of the updated and simulated forecast runs decreases during the forecast period. This is due to the formulation of the soil moisture accounting scheme (Eq. A.1) which is a stable dynamic system where small perturbations in the initial conditions vanish over time. For the second event, hence, the difference between the two runoff forecasts (with and without updating) is much smaller than for the first event in Fig. 9.

The previous figures have illustrated the temporal evolution of mean relative soil moisture. The model used is a distributed model where the model parameters are non-uniform in space and the inputs also differ spatially. The soil moisture is hence variable within the catchment. It is of interest to see how this spatial distribution changes with the updating. Fig. 10a shows a comparison of the spatial distribution of relative soil moisture within the catchment at the start of the forecast run on 15 August 2005 at 21 h (vertical line in Fig. 9). In this example, the updating increases mean relative soil moisture from 0.54 to 0.60 (Fig. 9) which is also apparent in Fig. 10a. It is mainly the mean that increases while the shape of the distribution does not change much. This spatial distribution indicates that most of the runoff stems from a relatively small portion of the catch-

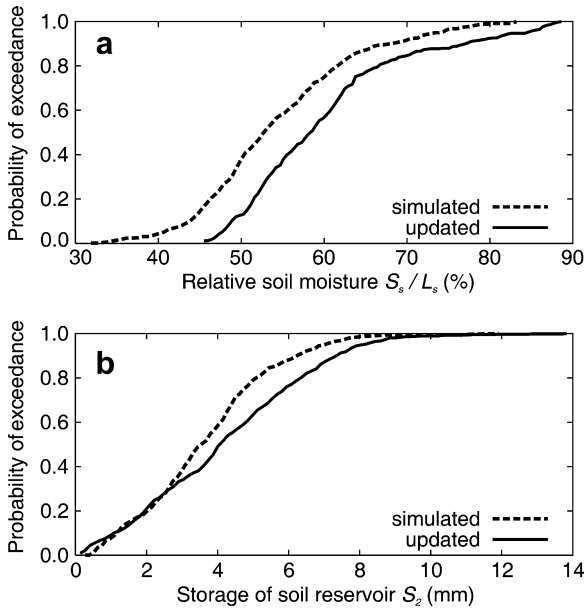

Figure 10 Spatial distributions of simulated and updated relative soil moisture S_s/L_s and soil storage S_2 on 15 August 2005 at 21 h at Zwettl/Bahnbrücke (622 km^2) used as initial conditions for the forecasts in Fig. 9.

ment with above soil moisture (Eq. A.1) and this spatial distribution is maintained in the updating. Indeed, the assumptions involve spatially uniform random errors $\varepsilon_{n,i}$ of precipitation and evaporation. Fig. 10b shows the corresponding spatial distribution of the storage of the soil reservoir S_2. This soil reservoir has a storage parameter k_2 that ranges between 6 and 17 days within the catchment, so represents an intermediate component in terms of the timing of runoff response. It is interesting that it is mainly the wetter parts of the catchment where the updating increases the soil storage, while the relatively dry parts remain almost unaffected. The wetter parts (larger S_2) are those that are hydrologically more active, and are also those that are more affected by the updating as one would expect.

Performance for large flood events

Most of the time, updating soil moisture leads to an improvement of the forecast accuracy. In particular, during low flow and average flow conditions the forecasts are very close to the data. However, the main interest in this paper is on flood forecasting, and in particular on the forecasting of large floods. The six largest flood events on record at the Kamp have hence been examined in more detail (Table 2). Some of these events are indeed extraordinary events. Flood records at the Kamp have been available since, 1977, and flood marks and archive information from the early 19th century. Based on this information, the largest flood on record (first event in August 2002) was assessed to be on the order of a 1000 year flood (Blöschl and Zehe, 2005). Some of the other floods are also large (second event in August 2002, about 500 years; March 2006 about ten years return period). The data set is hence particularly well suited to address the science question of whether the updating prior to events will actually improve the forecasts of large floods.

As in the previous analyses, two cases were examined, with and without updating soil moisture. In a first step the ability of the updating procedure to improve on the forecast of the flood peaks is examined. To this end, the forecasts are analysed that have been made 3 h before each flood peak occurred. For example, for the first event in August 2002, the flood peak occurred on August 8 at 0 h, so the forecast made on August 7, 21 h is analysed. Future precipitation was assumed to be known as in all the previous analyses, but no updating beyond the forecast time was allowed. The results of the comparison are shown in Fig. 11. For five out of the six flood events, the flood peaks are indeed improved. For example, the peak flow of the largest event was observed as 459 m^3/s while the forecast without and with updating soil moisture gives 508 and 470 m^3/s, respectively. The improvement of updating is larger for those events that are not represented so well in the simulation case. For the smallest event, the peak flow is slightly deteriorated (65 m^3/s observed and 56 and 53 m^3/s, respectively, without and with updating). The mean normalised absolute error of the peaks

$$e = \frac{1}{p}\sum_{k=1}^{p}\frac{|\widehat{Q}_k - Q_k|}{Q_k} \qquad (12)$$

was evaluated where Q_k are the observed flood peaks and $\widehat{Q}_k$ are the flood peak forecasts and $p = 6$. For the six peaks in Fig. 11 the mean normalised absolute error of the peaks is 25% without updating and decreases to 12% with updating. This is for a lead time of 3 h. For a lead time of 48 h the mean normalised absolute error of the peaks is 25% without updating and decreases to 19% with updating. It is clear, that overall, there are significant merits of the updating in terms of forecasting peak flows.

Table 2 Flood peaks, return periods and evaluation periods for the statistical error analysis of the six largest flood events on record at Zwettl/Bahnbrücke (622 km^2)

	August 2002a	August 2002b	July 2005	August 2005a	August 2005b	March 2006
Observed flood peak (m^3/s)	459	367	95	68	65	112
Return period of peak (yrs)	~1000	~500	5	3	3	10
Peak time	8 August, 0 h	13 August, 13 h	11 July, 10 h	16 August, 17 h	22 August, 8 h	31 March, 23 h
Beginning of entire event	6 August, 0 h	11 August, 0 h	5 July, 0 h	14 August, 0 h	20 August, 0 h	25 March, 0 h
End of entire event	10 August, 21 h	15 August, 21 h	15 July, 0 h	19 August, 21 h	26 August, 21 h	5 April, 12 h
Beginning of rising limb	6 August, 12 h	11 August, 12 h	10 July, 12 h	16 August, 0 h	21 August, 12 h	26 March, 6 h
End of rising limb	8 August, 6 h	13 August, 18 h	11 July, 6 h	17 August, 21 h	22 August, 12 h	2 April, 3 h

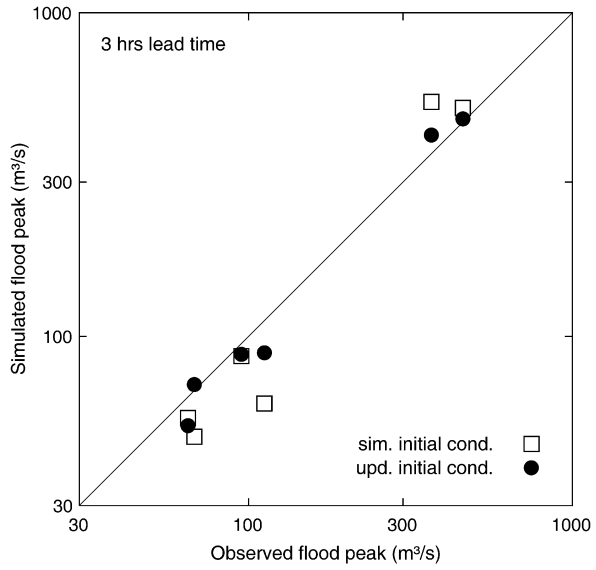

Figure 11 Comparison of the forecasted peak flows with and without updated initial conditions for the six largest flood events on record as of Table 2. Both forecast runs (updated and simulated) were started 3 h before the observed flood peaks (forecast lead time of 3 h) based on observed precipitation inputs.

In a second step, the forecast accuracy of the two cases is analysed for the entire events rather than the peaks only. Two error measures are used, the mean normalised absolute error e_j (Eq. 13) and the Nash-Sutcliffe efficiency E_j (Eq. 14):

$$e_j = \frac{1}{i_2 - i_1} \sum_{i=i_1}^{i_2} \frac{|\widehat{Q}_{ij} - Q_i|}{Q_i} \tag{13}$$

$$E_j = 1 - \frac{\sum_{i=i_1}^{i_2} (Q_i - \widehat{Q}_{ij})^2}{\sum_{i=i_1}^{i_2} (\overline{Q} - Q_i)^2} \tag{14}$$

where j is the forecast lead time, $\widehat{Q}_{ij}$ is runoff at time step i that is forecasted with a lead time of j, Q_i is the observed runoff at time step i, and i_1 and i_2 are the beginning and the end of the analysis interval, respectively (Table 2). In this analysis, the forecasts were made at 3 h intervals and different lead times of up to 48 h were analysed. We analysed two evaluation periods (i_1 to i_2); entire flood events, and the rising limbs only (see Table 2). The forecast errors for the entire events and the risings limbs are shown in Fig. 12a and b, respectively. In all instances, the updating of soil moisture reduces the forecast errors. For a lead time of 3 h, for example, the errors decrease from 20% to 12% in the case of the entire events, and 33% to 15% in the case of analysing the rising limbs only. For the case of simulated initial conditions, the forecast errors do not change with lead time as would be expected, as this is a simulation case where the forecast time does not come into play. In contrast, for the case of updated initial conditions, the errors are smallest for the short lead times, which again would be intuitively expected. At the time of the forecast, observed runoff at the time of the forecast captures some of the hydrological process dynamics that continue over the following hours. As the memory fades away with time, the improvement in forecast accuracy is largest for the short lead times. It is interesting that even after a forecast lead time of 48 h the updated initial conditions improve the forecasts substantially. Quite clearly, it is not only the fast runoff components that contribute to a given forecast accuracy.

The errors for the rising limbs (Fig. 12a) are generally larger than those for the entire flood events (Fig. 12b). This is because the forecast errors during the rising flood limbs are larger than those during the falling limbs due to rainfall uncertainty. During the falling limb rainfall is zero or very small, so rainfall uncertainty is small too. It is also possible, that the fast components of runoff are more uncertain than the slow components. Generally speaking, the rising limbs are more difficult to predict than the falling limbs but it

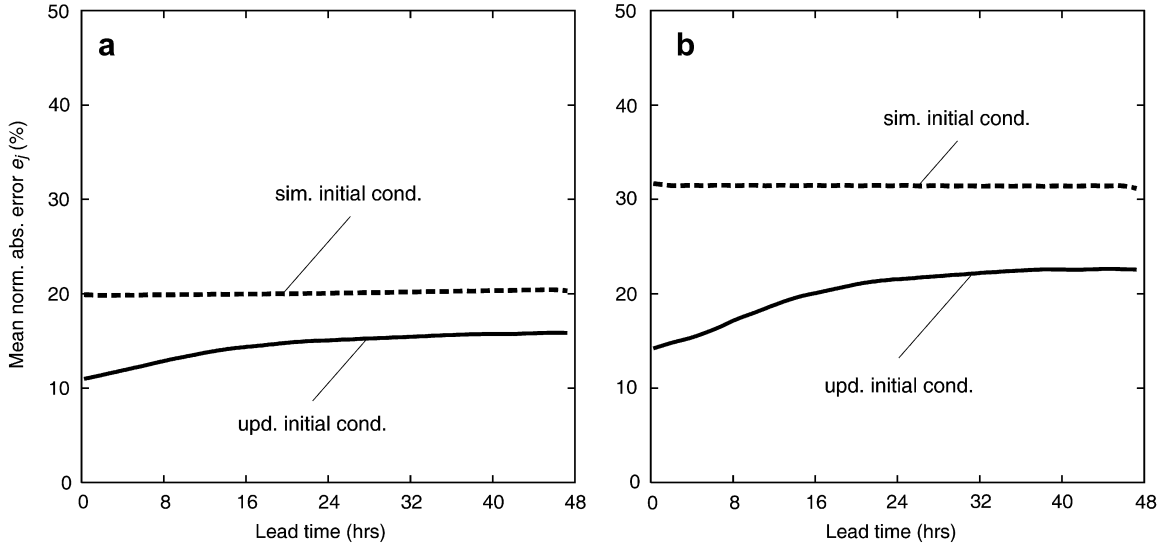

Figure 12 Forecast errors (Eq. (13)) for the six largest flood events on record (Table 2) assuming future precipitation is known. Dashed lines relate to the forecasts with simulated soil moisture (no-updating), solid lines to the forecasts with updated soil moisture. (a) Entire flood events; (b) rising limbs only.

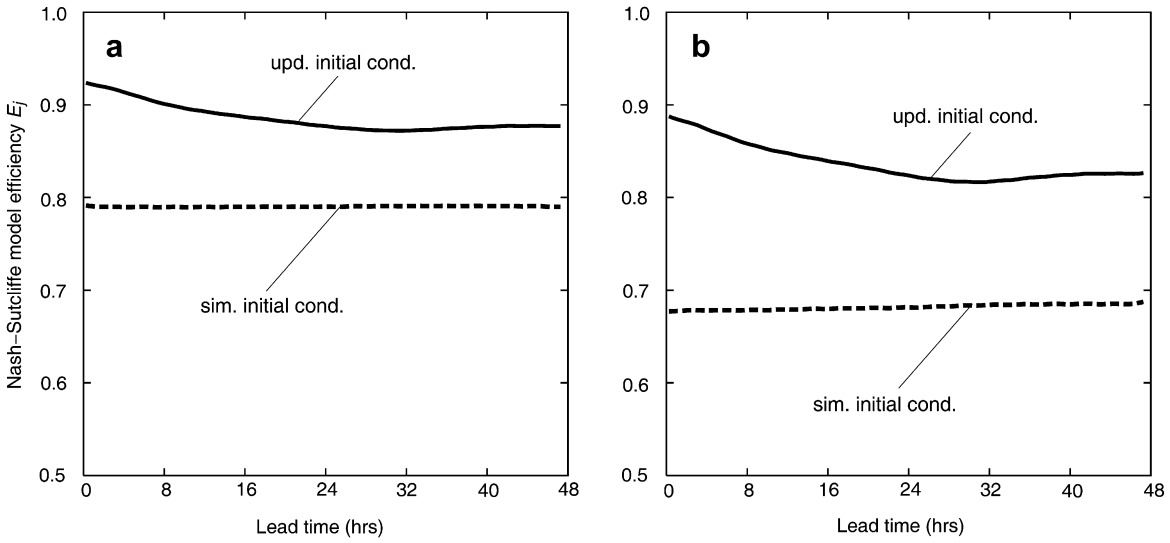

Figure 13 Nash-Sutcliffe model efficiency of the forecasts (Eq. (14)) for the six largest flood events on record (Table 2) assuming future precipitation is known. Dashed lines relate to the forecasts with simulated soil moisture (no-updating), solid lines to the forecasts with updated soil moisture. (a) Entire flood events; (b) rising limbs only.

are the former that are of most interest to flood management.

Fig. 13 shows the results of the Nash-Sutcliffe efficiency. This error measure involves squared errors (Eq. (14)), so the large deviations from the data are weighted more strongly than in the case of the mean absolute error. The error pattern of the Nash-Sutcliffe efficiency is similar to that of the mean absolute error. In both evaluation periods, rising limbs and entire flood events, the model efficiency is improved by the updating. For the entire flood events, the Nash-Sutcliffe efficiency at a forecast lead time of 48 h increases from 0.79 to 0.88 by the updating, and it increases from 0.79 to 0.92 at a lead time of 3 h. For the rising limbs, the Nash-Sutcliffe efficiency at a forecast lead time of 48 h increases from 0.68 to 0.82 by the updating, and it increases from 0.68 to 0.88 at a lead time of 3 h.

Discussion and conclusions

Renewed interest in updating methods in hydrology has come from the availability of Monte Carlo methods because of their flexibility, ease of use and operational robustness. The Ensemble Kalman Filter extends the traditional Kalman Filter concept by Monte Carlo techniques and is able to deal with non-linear model dynamics in a natural way. The aim of this paper is to examine the benefit of an updating procedure based on Ensemble Kalman Filter concepts in forecasting large floods. The soil moisture of a distributed runoff model is updated based on observed runoff. The updated soil moisture is then used as an initial condition for the forecasts. The ensemble size was set to $M = 10$ with $N = 10$ auxiliary realisations. Hardly any improvement in forecast accuracy was obtained when increasing the ensemble size in test simulations. A typical ensemble size used in the updating of hydrological models is 50 (Moradkhani et al., 2005). The advantage of the method proposed here is that it avoids calculation of the Jacobian that relates the states and the observations by using an iterative procedure of auxiliary realisations. The proposed method may be numerically less efficient than direct estimation of the Jacobian, depending on how it is calculated, but all the states of the model (soil moisture, ground water, snow) are fully consistent at all times. The main interest of this paper was, however, not in the particular formulation of the updating procedure but in the degree it will actually improve the forecasts for a real world case. During low and average flows the value of updating is usually obvious because of the long time scales associated with these hydrological processes. For large flood flows, the difficulty with updating runoff during an event is that phase errors usually cannot be handled well. There can be overshooting of the forecasts if phase errors are interpreted as volume errors. The procedure examined here mainly updates the slow runoff components, i.e., soil moisture between events which is then used as an initial condition for the flood forecasts. Sensitivity analyses and comparisons of individual events suggest that the concept of updating the slow component is plausible and robust. It is interesting that the non linearity of the rainfall-runoff model amplifies the small differences in runoff prior to the event. This means that small differences between simulated and observed hydrographs can have a great effect on the runoff forecast (Zehe and Blöschl, 2004). Conversely, these small differences can be exploited to improve the forecasts. The updating mainly changes the mean value of the catchment soil moisture, while the spatial structure of the moisture distribution is preserved during the update. Therefore, increasing catchment soil moisture leads to an increasing fraction of runoff contributing areas within the catchment. Analyses of six large flood events at the Kamp indicate that the updating indeed reduces forecast errors substantially during the flood events. It is considered a strength of this case study that data on a number of large floods (including two extreme floods) were available which is not usually the case in practical applications. This is important as one of the main motivations of implementing flood forecasting systems is to improve on the forecasting

of extreme events where the damage potential is largest (Apel et al., 2006).

Nash-Sutcliffe efficiencies of runoff models without updating reported in the literature are, typically, on the order of 0.7–0.9 (e.g., Parajka et al., 2005a). The efficiencies without updating found in this paper are at the lower end of this range (Fig. 13). It should be noted that low flow and average flow conditions can usually be simulated much more accurately than flood flows. For comparison, the Nash-Sutcliffe forecast efficiency at the Kamp was evaluated for entire years (as opposed to events) following an analogous procedure. The efficiencies without updating were always larger than 0.85 and increased to more than 0.98 if updating of soil moisture was allowed. Clearly, the updating is most efficient for low and medium flows, but from a practical perspective the flood flows are usually of much more interest. However, these tend to be more difficult to predict and errors are usually much larger. For example, a model comparison of Reed et al. (2004, their Fig. 18b) gave mean normalised absolute errors of peak flows in a typical range of 20–50%, depending on the model and the catchment analysed. Based on the results of this study, one would expect that such errors could be substantially reduced if soil moisture were updated. In the present paper, the peak flow errors for 3 h forecasts were reduced from 25% to 12% by the updating procedure, and from 25% to 19% for 48 h forecasts. It should be noted that the forecast lead time of 48 h is much larger than typical flow travel time in the streams within the catchment which are less than 2 h. It is hence the water in the landscape rather than that in the stream that needs to be adjusted in this case study.

Remotely sensed soil moisture is sometimes used for updating the soil moisture of hydrological models. The significant increase in forecast accuracy found here suggests that use of runoff data to infer catchment soil moisture may be an efficient alterative to remote sensing data. In fact, in the study area examined here it appears that updating soil moisture through observed runoff is a better choice than to directly use remotely sensed soil moisture data for updating (Parajka et al., 2005b).

The model parameters and structure were chosen very carefully in this case study. The model identification procedure went substantially beyond the calibration to runoff. Piezometric head data, and information from local surveys and other sources (such as snow data, Parajka and Blöschl, 2006) were used and combined by hydrological reasoning. This means that the model can be expected to represent the hydrological processes in the Kamp catchment reasonably well. We believe it is important to very carefully adjust the model to the local conditions (going beyond calibration to runoff) for the updating procedure to work efficiently. The events in 2005 and 2006 (Table 2) were not used for calibration but retained for model validation. In the current procedure, the main error source is attributed to the inputs (rainfall, evaporation) and their effect on soil moisture, so model parameters are not updated. A plausible model structure and carefully adjusted model parameters are hence the basis for a good performance of the updating routine. This is important as it then avoids the ''flogging a dead horse'' syndrome, i.e., attempting to update models that do not represent the processes well. Also, the availability of input data (16 rain gauges for model development, 8 telemetered rain gauges in a 622 km^2 catchment) along with radar data in this study is probably more than what one usually encounters in operational applications. With these caveats, it is suggested that updating procedures such as the one proposed in this paper can indeed substantially improve the forecasting of large floods at the catchment scale examined here.

Acknowledgements

Development of the forecasting model was funded by the State Government of Lower Austria and the EVN Hydropower company, Austria. Financial support of the EC (Project no. 037024, HYDRATE) is acknowledged. The authors would like to thank Dieter Gutknecht for numerous suggestions on this research, and two anonymous reviewers and Valentijn Pauwels for useful comments on the manuscript.

Appendix A. Structure of the soil moisture model

A conceptual soil moisture accounting scheme is used at the model grid scale. The sum of rain and melt from timestep i-1 to i, $P_{r,i/\,i-1} + M_{i/i-1}$, is split into a component $dS_{i/i-1}$ that increases soil moisture of a top layer, S_s, and a component $Q_{p,i/i-1}$ that contributes to runoff. The components are split as a function of $S_{s,i-1}$:

$$Q_{p,i/i-1} = \left(\frac{S_{s,i-1}}{L_s}\right)^{\beta} \cdot (P_{r,i/i-1} + M_{i/i-1}) \tag{A.1}$$

L_s is the maximum soil moisture storage. β controls the characteristics of runoff generation and is termed the non-linearity parameter. If the top soil layer is saturated, i.e., $S_{s,i-1} = L_s$, all rainfall and snowmelt contributes to runoff and $dS_{i/i-1}$ is 0. If the top soil layer is not saturated, i.e., $S_{s,i/i-1} < L_s$, rainfall and snowmelt contribute to runoff as well as to increasing S_s through

$dS_{i/i-1} > 0$:

$$\begin{aligned} dS_{i/i-1} &= P_{r,i/i-1} + M_{i/i-1} - Q_{p,i/i-1} - Q_{by,i/i-1} \quad \text{if } P_{r,i/i-1} \\ &\quad + M_{i/i-1} - Q_{p,i/i-1} - Q_{by,i/i-1} > 0 \\ dS_{i/i-1} &= 0 \qquad \text{otherwise} \end{aligned} \tag{A.2}$$

where, additionally, bypass flow $Q_{by,\,i/i-1}$ is accounted for. Analysis of the runoff data at the Kamp indicated that flow that bypasses the soil matrix and directly contributes to the storage of the lower soil zone is important for intermediate soil moisture states S_s. For

$\xi_1 \cdot L_s < S_{s,\,i-1} < \xi_2 \cdot L_s$ (with $\xi_1 = 0.4$, $\xi_2 = 0.9$) bypass flow was assumed to occur as

$$\begin{aligned} Q_{by,i/i-1} &= \alpha_{by} \cdot (P_{r,i/i-1} + M_{i/i-1}) \quad \text{if } \alpha_{by} \cdot (P_{r,i/i-1} + M_{i/i-1}) < L_{by} \\ Q_{by,i/i-1} &= L_{by} \qquad \text{otherwise} \end{aligned} \tag{A.3}$$

while no by pass flow was assumed to occur for dry and very wet soils. Changes in the soil moisture of the top soil layer S_s from time step $i-1$ to i are accounted for by

$$S_{s,i} = S_{s,i-1} + (dS_{i/i-1} - E_{A,i/i-1}) \cdot \Delta t \tag{A.4}$$

The only process that decreases S_s is evaporation $E_{A,i/i-1}$ which is calculated from potential evaporation, $E_{P,i/i-1}$, by a piecewise linear function of the soil moisture of the top layer:

$$E_{A,i/i-1} = E_{P,i/i-1} \cdot \frac{S_{s,i-1}}{L_p} \quad \text{if } S_{s,i-1} < L_p$$
$$E_{A,i/i-1} = E_{P,i/i-1} \quad \text{otherwise} \tag{A.5}$$

where L_p is a parameter termed the limit for potential evaporation. Potential evaporation was estimated by the modified Blaney-Criddle method (DVWK, 1996) as a function of air temperature. This representation of potential evaporation was compared to other methods in Parajka et al. (2003) suggesting that it gives plausible results in Austria.

References

Apel, H., Thieken, A.H., Merz, B., Blöschl, G., 2006. A probabilistic modelling system for assessing flood risks. Natural Hazards 38, 79–100.

Blöschl, G., Zehe, E., 2005. On hydrological predictability. Hydrological Processes 19 (19), 3923–3929.

Blöschl, G., Reszler, C., Komma, J., 2008. A spatially distributed flash flood forecasting model. Environmental Modelling & Software 23 (4), 464–478.

Crow, W.T., Van Loon, E., 2006. Impact of incorrect model error assumptions on the sequential assimilation of remotely sensed surface soil moisture. Journal of Hydrometeorology 7 (3), 421–432.

DVWK, 1996. Ermittlung der Verdunstung von Land- und Wasserflächen, DVWK-Merkblätter, Heft 238, Bonn.

Evensen, G., 1994. Sequential data assimilation with a nonlinear quasi-geostrophic model using Monte Carlo methods to forecast error statistics. Journal of Geophysical Research 99 (C5), 10,143–10,162.

Grayson, R., Blöschl, G., 2000. Spatial modelling of catchment dynamics. In: Grayson, R., Blöschl, G. (Eds.), Spatial Patterns in Catchment Hydrology: Observations and Modelling. Cambridge University Press, Cambridge, pp. 51–81 (Chapter 3).

Gutknecht, D., 1991. On the development of ''applicable'' models for flood forecasting. In: van de Ven, F.H.M., Gutknecht D., Loucks D.P., Salewicz, K.A. (Eds.), Hydrology for the Water Management of Large River Basins (Proceedings of the Vienna Symposium, August 1991), IAHS Publication No. 201, pp. 337–345.

Herschy, R.W., 2002. The uncertainty in a current meter measurement. Flow Measurement and Instrumentation 13, 281–284.

Kalman, R.E., 1960. A new approach to linear filtering and prediction problems. Transactions of the ASME – Journal of Basic Engineering 82 (D), 35–45.

Madsen, H., Rosbjerg, D., Damgard, J., Hansen, F.S., 2003. Data assimilation in the MIKE 11 Flood Forecasting System using Kalman Filtering. In: Blöschl, G. (Ed.), Water Resources Systems, vol. 281. IAHS publication, pp. 75–81.

Madsen, H., Skotner, C., 2005. Adaptive state updating in real-time river flow forecasting – a combined filtering and error forecasting procedure. Journal of Hydrology 308, 302–312.

McLaughlin, D., 1994. Recent advances in hydrologic data assimilation, In US National Report to the IUGG (1991–1994), Reviews of Geophysics, Supplement, pp. 977–984.

Merz, R., Blöschl, G., 2005. Flood Frequency Regionalisation – spatial proximity vs. catchment attributes. Journal of Hydrology 302 (1–4), 283–306.

Moradkhani, H., Sorooshian, S., Gupta, H.V., Houser, P.R., 2005. Dual state-parameter estimation of hydrological models using Ensemble Kalman Filter. Advances in Water Resources 28, 135–147.

O'Connell, P.E., Clarke, R.T., 1981. Adaptive hydrological forecasting – a review. Hydrological Sciences-Bulletin-des Sciences Hydrologiques 26, 179–205.

Parajka, J., Merz, R., Blöschl, G., 2003. Estimation of daily potential evapotranspiration for regional water balance modeling in Austria. In: 11th International Poster Day and Institute of Hydrology Open Day ''Transport of Water, Chemicals and Energy in the Soil – Crop Canopy – Atmosphere System, 20. November 2003, Bratislava, Slovakia. Published on CD-ROM, Slovak Academy of Sciences, ISBN 80-89139-02-7, pp. 299–306.

Parajka, J., Merz, R., Blöschl, G., 2005a. A comparison of regionalisation methods for catchment model parameters. Hydrology and Earth Systems Sciences 9, 157–171.

Parajka, J., Merz, R., Blöschl, G., 2005c. Regionale Wasserbilanzkomponenten für Österreich auf Tagesbasis (Regional water balance components in Austria on a daily basis) Österreichische Wasser- und Abfallwirtschaft, 57(H 3/4), pp. 43–56.

Parajka, J., Blöschl, G., 2006. Validation of MODIS snow cover images over Austria. Hydrology and Earth System Sciences 10, 679–689.

Parajka, J., Naeimi, V., Blöschl, G., Wagner, W., Merz, R., Scipal, K., 2005b. Assimilating scatterometer soil moisture data into conceptual hydrologic models at the regional scale. Hydrology and Earth System Sciences 10, 353–368.

Reed, S., Koren, V., Smith, M., Zhang, Z., Moreda, F., Seo, D.J., 2004. Overall distributed model intercomparison project results. Journal of Hydrology 298, 27–60.

Reichle, R., Dennis, McLaughlin, D., Entekhabi, D., 2002. Hydrologic data assimilation with the Ensemble Kalman Filter. Monthly Weather Review 130 (1), 103–114.

Reszler, Ch., Komma, J., Blöschl, G., Gutknecht, D., 2006. Ein ansatz zur identifikation flächendetaillierter abflussmodelle für die hochwasservorhersage (an approach to identifying spatially distributed runoff models for flood forecasting). Hydrologie und Wasserbewirtschaftung 50 (5), 220–232.

Weerts, A.H., Serafy, Y.H., 2006. Particle filtering and Ensemble Kalman Filtering for state updating with hydrological conceptual rainfall-runoff models. Water Resources Research 42. doi:10.1029/2005WR004093.

Wood, E.F., 1980. Real-time forecasting/control of water resources systems – selected papers from an IIASA workshop. In: IIASA Proceedings Series, vol. 8, pp. 37–46.

Zehe, E., Blöschl, G., 2004. Predictability of hydrologic response at the plot and catchment scales – the role of initial conditions. Water Resources Research 40, W10202.